Cancer Immunology, Immunotherapy (2022) 71:1497–1506
https://doi.org/10.1007/s00262-021-03098-w

ORIGINAL ARTICLE

Infiltration and Polarization of Tumor-associated Macrophages Predict Prognosis and Therapeutic Benefit in Muscle-Invasive Bladder Cancer

Mengmeng Sun[1] · Han Zeng[1] · Kaifeng Jin[1] · Zhaopei Liu[1] · Baoying Hu[2] · Chunnan Liu[1] · Sen Yan[1] · Yanze Yu[1] · Runze You[1] · Hongyi Zhang[1] · Yuan Chang[3] · Li Liu[4] · Yu Zhu[3] · Jiejie Xu[1] · Le Xu[5] · Zewei Wang[4]

Received: 30 June 2021 / Accepted: 20 October 2021 / Published online: 30 October 2021

Abstract

Background Muscle-invasive bladder cancer (MIBC) is an aggressive and heterogeneous malignancy. Tumor-associated macrophages (TAMs) are key infiltrating cell populations in the inflammatory microenvironment of malignant tumors including MIBC. It intrigues us to explore the clinical significance and immunoregulatory role of TAMs infiltration and polarization in MIBC.

Methods A total of 141 patients with MIBC from Zhongshan Hospital and 391 patients with MIBC from The Cancer Genome Atlas (TCGA) database were included in this study. Moreover, 195 patients who received anti-PD-L1 therapy from the IMvigor210 trial were enrolled. Patients were categorized into three subtypes considering the infiltration level and polarization status of TAMs, denoted as TAM^{low} (Subtype I), TAM^{high}&$M2/M1^{low}$ (Subtype II), and TAM^{high}&$M2/M1^{high}$ (Subtype III).

Results Subtype III suffered inferior prognosis, and Subtype II could benefit more from adjuvant chemotherapy (ACT). Subtype III was featured with increased pro-tumor cells and immunosuppressive cytokines, while Subtype II possessed more immunogenic cells infiltration with activated and tumoricidal properties. Subtype II and Subtype III presented basal/squamous-like characterization and showed additional prognostic merit beyond molecular classification. Subtype I exhibited elevated level of FGFR3 signature, while Subtype II had EGFR signaling activation and immunotherapeutic indication. Additionally, Subtype II patients were indeed highly sensitive to PD-L1 blockade therapy in IMvigor210 trial.

Conclusion The infiltration and polarization status of TAMs shaped distinct immune microenvironment with predictive significance for survival outcome, ACT benefit, and PD-L1 blockade therapy sensitivity in MIBC. Immune classification based on TAMs polarization and infiltration might provide tools to tailor chemotherapy and immunotherapy.

Keywords Tumor-associated macrophages · Muscle-invasive bladder cancer · Adjuvant chemotherapy · Immunotherapy · Tumor-immune microenvironment

Abbreviations

ACT	Adjuvant chemotherapy
AJCC	American Joint Committee on Cancer
CI	Confidence interval
CR	Complete response

Mengmeng Sun, Han Zeng, Kaifeng Jin, Zhaopei Liu: These authors contributed equally to this work.

✉ Jiejie Xu
jjxufdu@fudan.edu.cn

✉ Le Xu
xl11887@rjh.com.cn

✉ Zewei Wang
zwwang12@fudan.edu.cn

[1] Department of Biochemistry and Molecular Biology, School of Basic Medical Sciences, Fudan University, Shanghai 200032, China

[2] Department of Immunology, School of Medicine, Nantong University, Nantong, China

[3] Department of Urology, Fudan University Shanghai Cancer Center, Shanghai, China

[4] Department of Urology, Zhongshan Hospital, Fudan University, Shanghai, China

[5] Department of Urology, Ruijin Hospital, Shanghai Jiao Tong University School of Medicine, Shanghai 200025, China

CTLA-4	Cytotoxic T-lymphocyte-associated protein 4
EGFR	Epidermal growth factor receptor
FPKM	Fragments Per Kilobase of transcript per Million mapped reads
FGFR3	Fibroblast growth factor 3
GZMB	Granzyme B
HLA-DR	Human leukocyte antigen DR
HPF	High power field
HR	Hazard ratio
IC	Immune cells
ICIs	Immune checkpoint inhibitors
IFN-γ	Interferon γ
IHC	Immunohistochemistry
IL-10	Interleukin 10
LAG-3	Lymphocyte-activation gene 3
MIBC	Muscle-invasive bladder cancer
NAC	Neoadjuvant chemotherapy
NE	Not evaluated
NMIBC	Non-muscle-invasive bladder cancer
OS	Overall survival
PD	Progressive disease
PD-1	Programmed cell death protein 1
PD-L1	Programmed cell death ligand protein 1
PR	Partial response
PRF-1	Perforin 1
RC	Radical cystectomy
RFS	Recurrence-free survival
SD	Stable disease
TAMs	Tumor-associated macrophages
TC	Tumor cells
TCGA	The Cancer Genome Atlas
TGF-β	Transforming growth factor β
TIGIT	T-cell immunoreceptor with Ig and ITIM domains
TIM-3	T-cell immunoglobulin and mucin-domain containing-3
TMA	Tissue microarray analysis
TMB	Tumor mutation burden
TME	Tumor microenvironment

Précis

The framework based on TAMs infiltration and polarization was identified as an independent predictor for the prognosis of MIBC patients, which was associated with sensitivity to adjuvant chemotherapy, and PD-L1 inhibitor.

Introduction

Bladder cancer is one of the most common urogenital malignancies around the world, which could be further classified into non-muscle-invasive bladder cancer (NMIBC) and muscle-invasive bladder cancer (MIBC) [1, 2]. Compared to NMIBC, patients diagnosed with MIBC often have rapid progression, metastasis, and worse overall prognosis [3, 4]. Radical cystectomy (RC) with lymph node dissection, preceded by cisplatin-based neoadjuvant chemotherapy (NAC), remains the current standard first-line treatment settings for MIBC [5]. Adjuvant chemotherapy (ACT) should be considered for some patients if no NAC efficacy occurs [6]. Lamentably, more than half of patients with MIBC, which develop specific recurrence and the five-year survival rate have not been significantly improved [6, 7]. Several new therapeutic options have expanded to include antibody–drug conjugates, immune checkpoint inhibitors (ICIs), and targeted therapies in recent years [8, 9], while they showed limited efficacy in MIBC. Therefore, efficacious and well-tolerated predictive biomarkers for patients' therapeutic response are urgently needed to be explored in MIBC.

Tumor-associated macrophages (TAMs), highly presented in the microenvironment of solid tumors, are featured with the capacity for functional plasticity. Based on their distinct functional abilities, TAMs can be divided into two different states, M1-like and M2-like [10]. Established evidence denotes that in nascent tumors, TAMs display an M1-like activity, which can clear some immunogenic tumor cells [11]. Along the course of cancer continues, M1-like TAMs are often derived toward an anti-inflammatory and pro-tumor M2-like phenotype [12]. Thus, the complexity of TAMs would be better described as a dynamic spectrum of phenotypes in response to signals in tumor microenvironment (TME) rather than a fixed status [13]. The model of polarization of different macrophage phenotypes, which is associated with reduced host defense and chronic infection, is propitious for us to comprehend its trajectory in TAMs. Our previous studies have pointed that a weighted complex immune network including TAMs infiltration was correlated with clinical outcomes in MIBC [14], and uncovered the carcinogenic role of specific TAMs population expressing lectins [15, 16], highlighting TAMs contribution in immunosuppressive microenvironments in MIBC. However, the clinical significance of framework based on TAMs infiltration and polarization failed to be systematically explored in MIBC.

In this study, we identified a population of MIBC patients with poor prognosis, suboptimal ACT responsiveness, and immunosuppressive contexture according to the infiltration and polarization of TAMs. Additionally, immune classification based on TAMs infiltration and polarization was associated with sensitivity to PD-L1 blockade immunotherapy and could refine patients clinical outcomes coupled with molecular classification. Our work offers a novel perspective on the essential role of TAMs in programming the tumor-immune microenvironment and therapeutic landscape in MIBC.

Methods and materials

Patients' enrollment

Three independent cohorts, *Zhongshan Hospital* (ZSHS, surgery date: 2002–2014) cohort, *the Cancer Genome Atlas* (TCGA) cohort, and *IMvigor210* cohort, were included in this study. The ZSHS cohort comprised 215 patients receiving radical cystectomy, and 141 of them met the inclusion criteria: (a) informed consent; (b) full details of clinicopathologic data; (c) pathological diagnosed as MIBC (13 nonurothelial carcinomas; 60 pathological Ta/ Tis/ T1); (d) received cisplatin-based ACT and RC therapies only; (e) without detachment in the tissue microarray analysis (TMAs) (one case excluded) [17]. Overall survival (OS) and recurrence-free survival (RFS) were calculated as intervals from the date of cystectomy to death or first relapse (regardless of any cause). Informed consent was obtained from all the patients, and the study was approved by the Clinical Research Ethics Committee of Zhongshan Hospital.

A total of 412 patients from TCGA database were also enrolled in this study. Twenty-one patients were excluded due to the deficiency of survival data ($n = 3$), lack of sequencing data ($n = 4$), NMIBC pathologic diagnoses ($n = 4$), and receiving neoadjuvant therapy ($n = 10$). Supplementary Table 1 showed the demographics and clinicopathological characteristics of patients with MIBC in ZSHS and TCGA cohort. The flowchat of study population from two cohorts was illustrated in Supplementary Fig. 1A.

A large phase 2 trial (IMvigor210) was designed to investigate the clinical activity of PD-L1 blockade with atezolizumab in metastatic urothelial cancer (mUC) [18]. A total of 195 patients out of 348 patients who accepted PD-L1 blockade therapy (atezolizumab) were included for bladder-derived urothelial carcinoma in IMvigor210 cohort to verify predictive effectiveness of our latent promising immune stratification.

mRNA expression data and processing

We used Fragments Per Kilobase of transcript per Million mapped reads (FPKM) to calculate the relative transcript level of genes, and the mRNA expression of patients from TCGA and IMvigor210 cohort was standardized via formula $\log_2$ (FPKM + 1) before analyses. The involved signatures were scored as the average of related genes expression (Supplementary Table 2). Besides, molecular subtype information of patients was derived using R package BLCA subtyping (https://github.com/cit-bioinfo/BLCAsubtyping). Genomic, transcriptomic, and matched clinical data from IMvigor210 cohort were downloaded from http://research-pub.gene.com/IMvigor210CoreBiologies [19].

Tissue microarray and immunohistochemistry

Formalin-fixed, paraffin-embedded tissue samples of representative tumor regions of ZSHS cohort were used for the TMAs construction. TMAs are from one original patient cohort of 215 patients from Zhongshan Hospital, Fudan University. In this study, TMAs were manufactured at Shanghai Outdo Biotech Co., Ltd (Shanghai, China). We subjected these tissue sections to H&E staining for histological verification to ensure the presence of available tumor tissue. Sections from the TMAs blocks were cut at 4 μm.

The immunohistochemistry (IHC) protocol has been described previously [20]. For double immunohistochemistry, the TMAs slides were baked at 60℃ for 6 h, deparaffinized with xylene, and rehydrated through graded alcohol series. Antigen retrieval was performed in autoclave heating using 0.01 M sodium citrate buffer (pH 6.0) for 7 min. Samples were then incubated with anti-HLA-DR antibody overnight at 4℃, followed by incubation alkaline phosphatase (AP)-labeled (goat anti-rabbit IgG) antibody in blocking buffer for 1 h at room temperature. Visualization was completed with Vector Blue. Subsequently, TMAs were washed and incubated with anti-CD68 antibody for 2 h at 37 °C. After washing, bound antibodies were then detected with the secondary horseradish peroxidase (HRP)-labeled antibody (goat anti-mouse IgG) and diaminobenzidine (DAB) substrate. Images were collected on a DM6000 B Leica microscope. Immune cells were stained with corresponding antibodies as summarized in Supplementary Table 3. CD68 was used as pan-macrophage marker, and CD206 was identified as M2 macrophages marker. CD68 combined with HLA-DR were applied to detect M1 macrophages infiltration [21]. Representative images of different types of macrophages were shown in Supplementary Fig. 1B. Besides, CD56 was a functional marker for the identification of NK cells [22]. Naive $CD4^+$ T cells were differentiated into Th1 or Th2 cells, which respectively expressed T-bet and GATA3 as specific differentiation markers [23, 24]. Mast cells were perceived using anti-mast cell tryptase [17]. Moreover, CD66b was specifically displayed neutrophils surface as molecular biomarker [25]. HLA-DR combined with CD11c were used to detect dendritic cells [17].

Immune cells evaluation and cut-off value

To assess the infiltration of immune cells, the evaluation was taken from three random areas of tumor tissue. All stains were scored independently by two pathologists who were blinded to clinical diagnosis. The mean count of their evaluation was adopted. For the cases with discordant results exceeded 5 cells, the two pathologists read the slides again together to get a concordance. Through mRNA data obtained from TCGA (https://tcga-data.nci.nih.gov/tcga/) and IMvigor210 cohort, CIBERSORT web tool (http://cibersort.stanford.edu/) was utilized to estimate the absolute proportions of LM22 human immune cell subclasses. The level of TAMs was calculated by summing macrophages M0, M1, and M2 in TCGA and IMvigor210 cohorts. Top 48% TAMs were defined as high infiltration (> 27 cells/HPF), and the rest of patients were uniformly assigned to TAMs low infiltration group (≤ 27 cells/ HPF) according to the minimum log-rank *P* -value in ZSHS cohort. Top 37% M2/M1 ratio was regarded as high (cut-off value was 2.88), which is determined by X-tile 3.6.1 (Yale University). These patients' proportion of stratification based on TAMs infiltration and polarization was applied in the TCGA cohort and IMvigor210 cohort for consistency.

Statistical analysis

Results were presented as median (quartiles). The Pearson χ^2 test or adjusted χ^2 test was applied for analysis of categorical variables, and a nonparametric test (Mann–Whitney U test) was performed for continuous variables. And the correlation between different variables employed Spearman correlation to evaluate. The survival curves were generated by Kaplan–Meier method and analyzed using the log-rank test. Univariate and multivariate analyses were also conducted using the Cox proportional hazards regression model and 95% confidence intervals. Statistical analyses were conducted using SPSS 26.0, R 3.6.1. All statistical analyses were two-sided, and $P < 0.05$ was regarded as statistically significant.

Results

Correlation of immune stratification based on TAMs infiltration and M2/M1 ratio with clinical outcomes in MIBC

According to previous studies, increased TAMs infiltration was correlated with the poor prognosis of muscle-invasive bladder cancer [5]. The tumor microenvironment promotes the generation of immunosuppressive and protumorigenic macrophage M2 polarization. Hence, we analyzed the clinical correlation of infiltration and polarization of TAMs in MIBC. We analyzed prognostic implication of M2/M1 ratio according to TAMs infiltration in ZSHS cohort and uncovered that M2/M1 ratio was correlated with inferior survival in a TAMs infiltration-dependent manner (Supplementary Fig. 2). Therefore, we categorized patients into three subtypes: TAM^{low} (Subtype I), TAM^{high}&$M2/M1^{low}$ (Subtype II), and TAM^{high}&$M2/M1^{high}$ (Subtype III) (Supplementary Fig. 1C). To further elucidate the clinical significance of TAMs infiltration and M2/M1 ratio, Kaplan–Meier curves were conducted to compare the prognosis among MIBC patients. In ZSHS cohort, we observed Subtype II appeared to have the lowest survival rates (OS: 5-year survival rates: 36.9%, $P = 0.0017$; RFS: 5-year survival rates: 23.4%, $P = 0.0135$; Fig. 1A). We use CIBERSORT to deconvolute the transcriptome of TCGA Bulk RNA-Seq samples into the likely constituent cell types. Meanwhile, immune classification based on immune cells density was parallelly constructed in TCGA cohort, which was consistent with the findings in histologic settings of ZSHS cohort (OS: $P = 0.0039$, RFS: $P = 0.0043$; Fig. 1B). Following these results, we then conducted univariate and multivariate analyses to determine whether immune class based on TAMs infiltration and M2/M1 ratio are independent of other variables (Supplementary Fig. 1D, Fig. 1C). The outcomes identified that immune class based on TAMs infiltration and M2/M1 ratio could be served as an independent prognostic factor for OS and RFS to predict survival of patients with MIBC.

Predictive merit of immune stratification based on TAMs infiltration and M2/M1 ratio with response to cisplatin-based adjuvant chemotherapy in MIBC

ACT has been widely used in the treatment of patients with MIBC. However, patients who received cisplatin-based ACT failed to show a long-term survival benefit in previous studies, which was also detected in ZSHS cohort (Fig. 2A and B) [15]. Interestingly, Subtype II had significantly longer OS and RFS after ACT application (OS: $P = 0.0311$, RFS: $P = 0.0383$; Fig. 2C and D), while patients failed to exhibit survival benefit from ACT in Subtype I and Subtype III. *P* interaction according to cox regression analysis further validated that our novel classification could effectively distinguish patients who respond to ACT ($P = 0.036$, $P = 0.012$, Fig. 2C and D). Patients from TCGA cohort were omitted for data missing and the indeterminacy of chemotherapeutic agents.

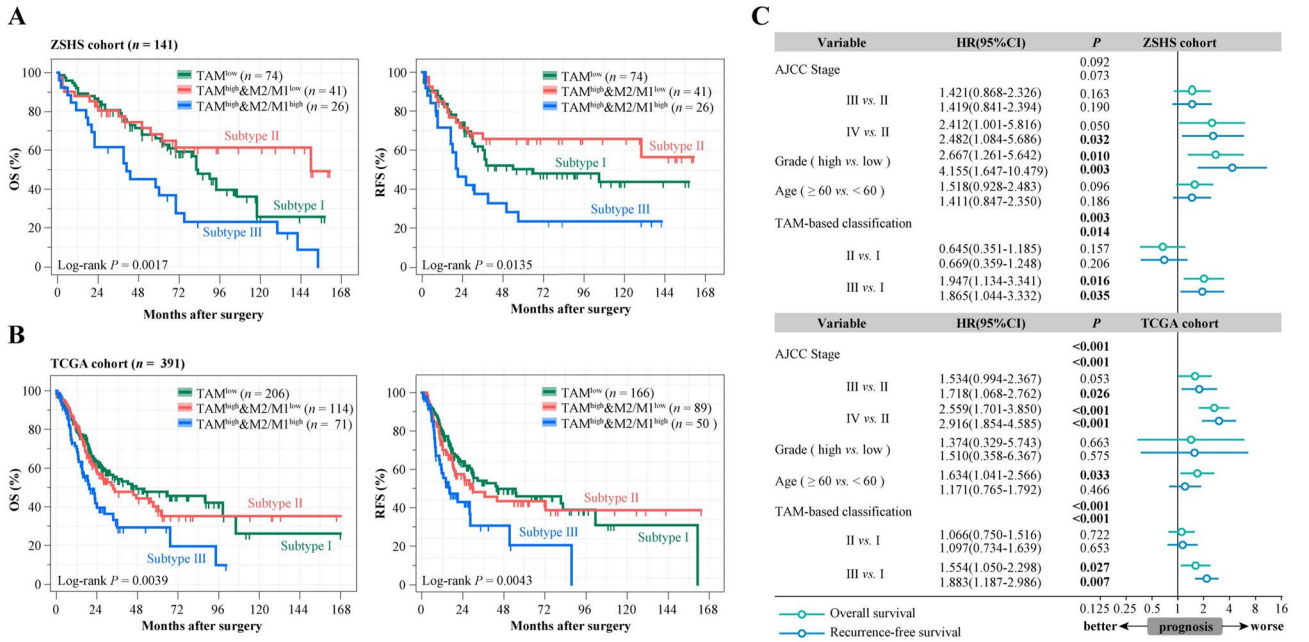

Fig. 1 Correlation of immune stratification based on TAMs infiltration and M2/M1 ratio with clinical outcomes in MIBC. **A-B** Kaplan–Meier curves of OS (left) and RFS (right) in ZSHS cohort **A** and TCGA cohort **B** based on TAMs infiltration and M2/M1 ratio. *P* values were calculated by log-rank test. **C** Multivariate Cox analysis of clinicopathological characteristics and immune stratification based on TAMs infiltration and M2/M1 ratio in ZSHS and TCGA cohort. OS, overall survival; RFS, recurrence-free survival; CI, confidence interval; HR, hazard ratio; AJCC, American Joint Committee on Cancer

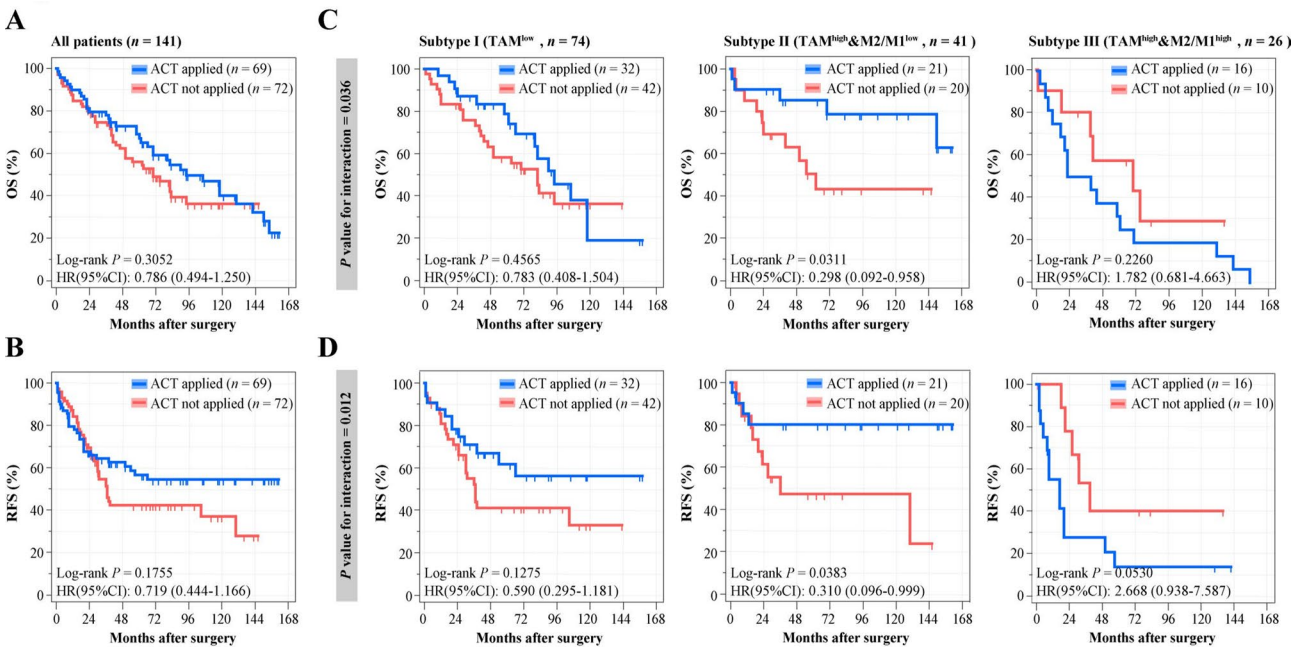

Fig. 2 Predictive merit of immune stratification based on TAMs infiltration and M2/M1 ratio with response to cisplatin-based adjuvant chemotherapy in MIBC. **A-B** Kaplan–Meier curves estimates of OS **A** and RFS **B** stratified according to ACT application in ZSHS cohort. **C-D** Kaplan–Meier curves for OS **C** and RFS **D** stratified according to ACT application combined with TAMs infiltration and M2/M1 ratio. Data were analyzed by log-rank test

Stratification based on TAMs infiltration and M2/M1 ratio trichotomies distinct TME features in MIBC

To investigate the immune mechanism for the prognosis stratification preliminarily, we attempted to characterize the immune contexture in immune classification based on TAMs infiltration and M2/M1 ratio. After evaluating the association of three subtypes with 19 immune cell types (CIBERSORT algorithm) in TCGA cohort, we found that Subtype II had more immunogenic cells infiltration, while Subtype III showed elevated pro-tumor-immune cells (Fig. 3A). To validate the results derived from the TCGA cohort, we further conducted IHC staining of immune cells on the TMA from the ZSHS cohort (Fig. 3B, Supplementary Fig. 3A–E). Subtype II consistently showed anti-tumorigenic immune cells abundance ($CD8^+$ cells, NK cells, T-helper 1 cells; Fig. 3B, top panel). Additionally, mast cells, neutrophils, and T-helper 2 cells were recruited in the tumor microenvironment and facilitated tumor-mediated immune escape in Subtype III (Fig. 3B, bottom panel) [26]. Likewise, Subtype II was associated with a higher level of immune checkpoint and effector molecule expression, yet Subtype III showed elevated immune inhibitory molecules in TCGA cohort (Fig. 3C). Our histochemistry results in ZSHS cohort also confirmed the above results. (Fig. 3D-F). We explored the relationship between PD-L1 distribution and our immune

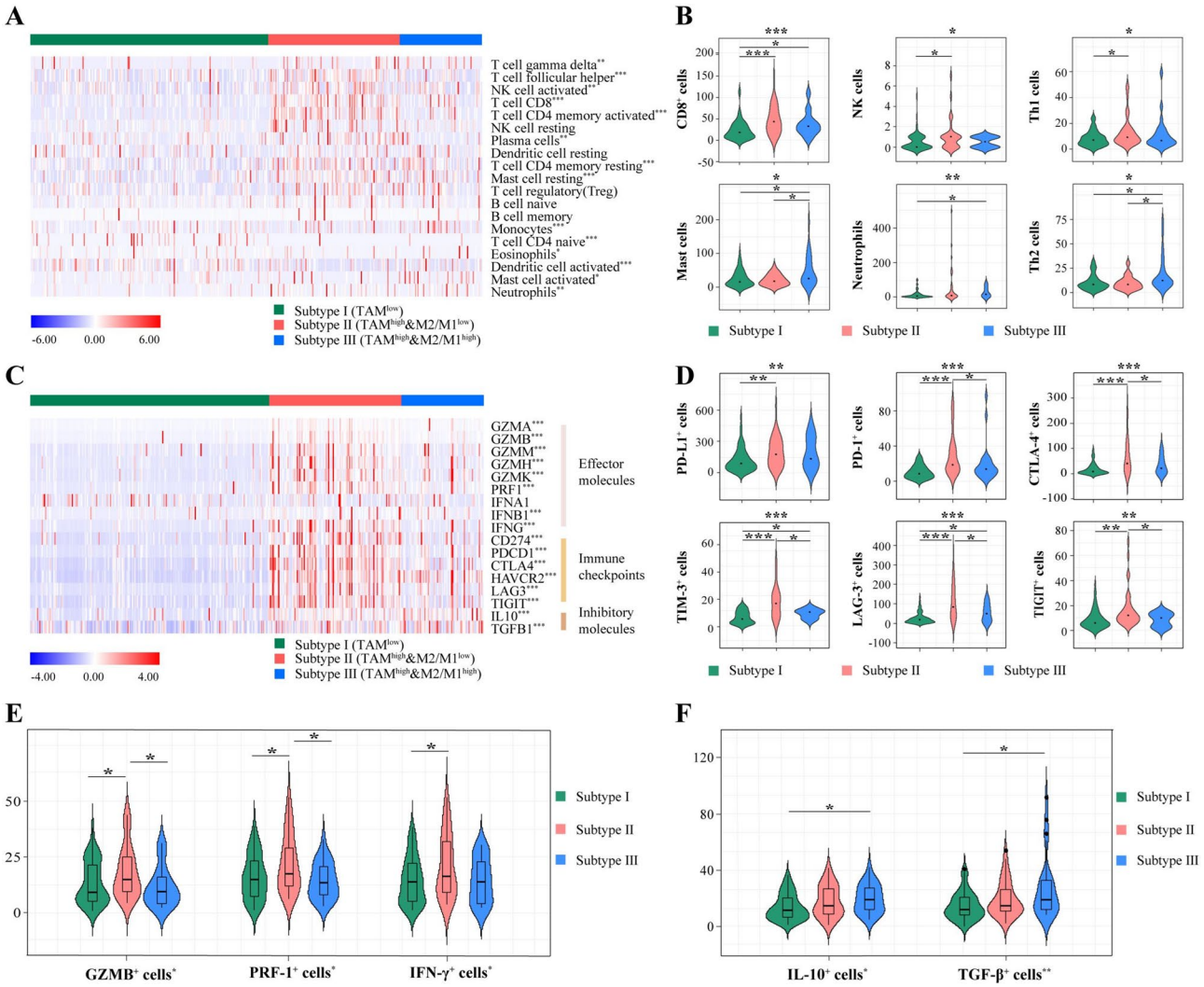

Fig. 3 Stratification based on TAMs infiltration and M2/M1 ratio trichotomized distinct TME features in MIBC. **A** Heatmaps of immune cells infiltration with immune stratification in TCGA cohort. **B** Association between immune stratification and immune cells infiltration assessed by IHC staining in ZSHS cohort. **C** Heatmaps of gene expression involved in multiple immune response with immune stratification in TCGA cohort. **D-F** Association of immune stratification with immune checkpoint **(D)**, effector cytokines **(E)**, and immunosuppressive cytokines **(F)** expression assessed by IHC staining in ZSHS cohort. Data were analyzed by Kruskal–Wallis test. $*P<0.05$, $**P<0.01$ and $***P<0.001$

stratification in IMvigor210 cohort. It was observed that Subtype II was significantly associated with higher PD-L1 immune cells (IC) level and tumor cells (TC) level, while PD-L1 TC was accumulated in Subtype III ($P < 0.001$; Supplementary Fig. 3F).

Conclusively, Subtype II with M1 polarized characteristics conferred an immune-activated TME with function in eliminating the abnormal cells. Subtype III with M2 polarized features showed ubiquitous immune evasion with immunosuppressive cells and molecules expression, and Subtype I displayed immune-desert phenotype. These results were largely in line with the infiltration and polarization of TAMs, which shaped the dynamic phenotypes in response to signals at the tumor microenvironment.

Molecular and therapeutic implications across immune stratification based on TAMs infiltration and M2/M1 ratio

Mounting studies indicated that molecular features of MIBC have yielded a promising avenue for prognostic stratification and individualized therapy [27]. We found that the immune stratification based on TAMs infiltration and M2/M1 ratio significantly correlated with molecular subtypes in MIBC. Remarkably, Subtype II and Subtype III were accumulated in basal-squamous subtypes according to both Consensus and TCGA 2017 classification ($P < 0.001$, $P < 0.001$; Fig. 4A). Similarly, we found that Subtype II and Subtype III showed a high basal signature score, while Subtype I contained the elevated luminal signature score ($P < 0.001$, $P < 0.001$; Supplementary Fig. 4A). Both in Ba/Sq subtype of Consensus and TCGA 2017 classification, Subtype III had worse overall survival ($P = 0.0479$, $P = 0.0516$; Fig. 4B). These results were further confirmed

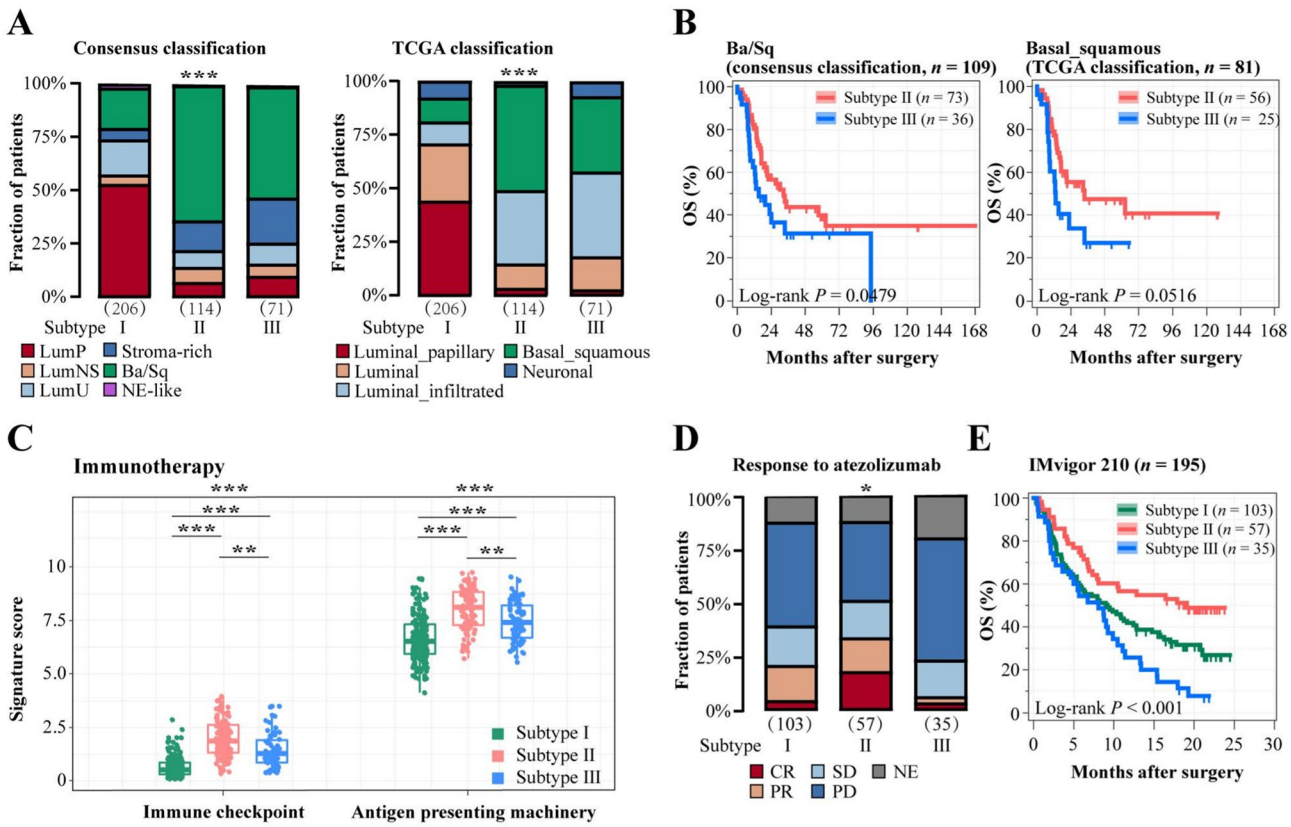

Fig. 4 Molecular and therapeutic implication across immune stratification based on TAMs infiltration and M2/M1 ratio. **A** Quantification analyses of TAMs infiltration and M2/M1 ratio across molecular classification systems in TCGA cohort. **B** Kaplan–Meier curves for OS stratified according to immune stratification in basal/squamous patients (left: consensus classification; right: TCGA classification). **C** Immunotherapy signature score with immune stratification based on TAMs infiltration and M2/M1 ratio. **D** Relationship between response to atezolizumab and immune stratification. **E** Kaplan–Meier curves of OS based on TAMs infiltration and M2/M1 ratio in IMvigor210 cohort. Data were analyzed by Kruskal–Wallis test and log-rank test. *$P < 0.05$, **$P < 0.01$ and ***$P < 0.001$. CR, complete response; PR, partial response; SD, stable disease; PD, progressive disease; NE, not evaluated

in IMvigor210 ($P < 0.001$, $P = 0.0393$; Supplementary Fig. 4B). It has been well-documented that the promising efficacy of fibroblast growth factor 3 (FGFR3) inhibitor and epidermal growth factor receptor (EGFR) inhibitor in MIBC patients [28, 29]. We discovered that Subtype I presented a high level of FGFR3 signal activation signature score, which might be sensitive to FGFR3-targeted therapies ($P < 0.001$, $P = 0.002$; Supplementary Fig. 4C). We observed Subtype II exhibited activated EGFR signaling and immunologic pathway ($P < 0.001$, $P < 0.001$; Fig. 4C and Supplementary Fig. 4D), which implied its positive correlations with the efficacy of EGFR-targeted therapy and immunotherapy. Targeting PD-L1 pathway could induce robust and durable immunotherapy responses in patients with various cancers including bladder cancer [30]. We used samples from the IMvigor210 trial to validate therapeutic implication across immune stratification based on TAMs infiltration and M2/M1 ratio. Intriguingly, Subtype II was significantly associated with durable response to PD-L1 blockade, while Subtype III was related to the anti-PD-L1 resistance ($P = 0.028$; Fig. 4D). Subtype II showed the best overall survival after atezolizumab application in IMvigor210 trial ($P < 0.001$; Fig. 4E). Besides, through multivariate Cox analysis, our classification was independent on PD-L1 IC, but not tumor mutation burden (TMB) level to predict clinical risk of patients receiving PD-L1 inhibitors in IMvigor210 cohort (Supplementary Table 4–5). Collectively, our immune stratification based on TAMs infiltration and M2/M1 ratio redefined clinical implications of molecular subtypes and further discriminated responsiveness to PD-L1 blockade therapy in MIBC.

Discussion

Instead of focusing on the biological status of tumor cells, increasing attention has recently been directed toward the TAMs, which play an important role in promoting tumor proliferation and regulating anti-tumor immunity in TME [31]. In solid tumors, TAMs polarization impacted patient's clinical outcomes and the effectiveness of systematic therapies, which make it a potential candidate for novel cancer target therapy [21, 32]. Despite advances in surgical and medical therapy, the prognosis for patients with MIBC remains largely unchanged over the past several decades [33]. Accurate prognostic evaluation is essential for clinical decision making, determining the prognosis and selection of treatment intervention. Thus, in this research, we found that infiltration and polarization of TAMs correlated with prognosis and therapeutic benefit in MIBC. Further analysis indicated that Subtype III with M2 polarized features conferred poor prognosis, inferior ACT efficacy, and PD-L1 blockade responsiveness of MIBC patients. These findings highlighted the importance of TAMs infiltration and polarization as a potential prognostic and predictive marker for MIBC.

Chemoresistance is the main obstacle in patients receiving ACT therapy, and the immunosuppressive status could determine ineffective treatment occurrence [20]. Tumors with TAMs infiltration and M2-like polarization marked an immunosuppressive contexture with tumorigenic immune cells and immunosuppressive cytokines abundance. Subtype II showed more cells with immunogenic and tumoricidal properties, which could provide a reasonable explanation for their chemotherapy efficacy diversity. Besides, Subtype II and Subtype III also displayed remarkable dissimilarity regarding the response of PD-L1 therapy. Patients in Subtype II with more immune-activated pathways showed better responses to PD-L1 blockade. The above results suggested that the infiltration and polarization of TAMs not only impacted clinical outcomes and immune microenvironment for patients but also differentiated therapeutic susceptibility. The infiltration and polarization of TAMs might be served as a companion diagnostic marker for precision treatment options.

Recently, transcriptome profiling and genomic data facilitate MIBC classification into various molecular subtypes, which could unmask tumor biological properties and guide therapeutic options [34]. MIBC molecular subtypes are broadly grouped into basal and luminal subtypes, showing similarities to the molecular phenotypes of breast cancer [35]. We found that M2 polarization coupled with high level of TAMs positively associated with basal/squamous-like characterization. It has been shown that basal/squamous subtype is associated with poor response, immune cell infiltration, and high PD-1 protein expression, which failed to distinguish the efficacy of immune checkpoint inhibitors and other immunotherapies [36, 37]. Meanwhile, macrophages constitute a principal component of the immune infiltrates in solid tumors by differentiating into TAMs. Interestingly, basal-featured patients with elevated M1 macrophages possessed better response to immunotherapy, while M2 macrophages infiltration potentially promoted immunotherapeutic resistance in basal-featured patients. These findings of macrophages heterogeneity in basal/squamous subtypes might explain the phenomenon that those basal-like patients characterized by high immune infiltration failed to obtain survival benefits from PD-L1 blockade. Future studies could develop therapeutic strategies based on reprogramming TAMs combined with PD-L1 inhibitors to reinforce an anti-tumor immunity in basal-featured MIBC patients. Therefore, our novel immune stratification based on TAMs infiltration and polarization was crucial for refining the prognostic value of molecular subtypes in MIBC.

In summary, TAMs polarization and infiltration might serve as an independent prognostic indicator and predictive marker for the efficacy of systemic therapies including ACT and PD-L1 inhibitors, which is worth further investigating its potential role as a systemic companion biomarker in prospective studies of MIBC.

Supplementary Information The online version contains supplementary material available at https://doi.org/10.1007/s00262-021-03098-w.

Acknowledgements We thank Dr. Lingli Chen (Department of Pathology, Zhongshan Hospital, Fudan University, Shanghai, China) and Dr. Yunyi Kong (Department of Pathology, Fudan University Shanghai Cancer Center, Shanghai, China) for their excellent pathological technology help.

Authors' contributions M. Sun, H. Zeng, K. Jin, and Z. Liu involved in acquisition of data, analysis and interpretation of data, statistical analysis, and drafting of the manuscript; C. Liu, S. Yan, Y. Yu, R. You, H. Zhang, Y. Chang, Y. Wang, L. Liu, and Y. Zhu involved in technical and material support; J. Xu, L. Xu, and Z. Wang involved in study concept and design, analysis and interpretation of data, drafting of the manuscript, and obtained funding and study supervision. All authors read and approved the final manuscript.

Funding This study was funded by grants from National Natural Science Foundation of China (31770851, 81872082, 82002670, 82103408), Shanghai Municipal Natural Science Foundation (19ZR1431800), Shanghai Sailing Program (18YF1404500, 21YF1407000), Shanghai Municipal Commission of Health and Family Planning Program (201840168) and Fudan University Shanghai Cancer Center for Outstanding Youth Scholars Foundation (YJYQ201802). All these study sponsors have no roles in the study design, in the collection, analysis, and interpretation of data.

Data availability All data generated that are relevant to the results presented in this article are included in this article. Other data that were not relevant for the results presented here are available from the corresponding author Prof. Xu upon reasonable request.

Declarations

Conflict of interest The authors declare that they have no competing interests.

Ethics approval The study was approved by the Clinical Research Ethics Committee of Zhongshan Hospital, Fudan University, with the approval number Y2015-054. Written informed consent was obtained from each patient included and this study was performed under the Declaration of Helsinki. Signed informed consent was obtained from each patient.

Consent for publication All authors provide their consent for publication.

Study approval This study was approved by the Clinical Research Ethics Committee of Zhongshan Hospital, Fudan University (No. B2015-030). Written informed consent was obtained from each patient.

References

1. Sanli O, Dobruch J, Knowles MA, Burger M, Alemozaffar M, Nielsen ME et al (2017) Bladder cancer Nat Rev Dis Primers 3:17022
2. Johnson SB, Yu JB (2018) Bladder preserving trimodality therapy for muscle-invasive bladder cancer. Curr Oncol Rep 20:66
3. Chou R, Selph SS, Buckley DI, Gustafson KS, Griffin JC, Grusing SE et al (2016) Treatment of muscle-invasive bladder cancer: a systematic review. Cancer 122:842–851
4. Taylor J, Becher E, Steinberg GD (2020) Update on the guideline of guidelines: non-muscle-invasive bladder cancer. BJU Int 125:197–205
5. Schneider AK, Chevalier MF, Derre L (2019) The multifaceted immune regulation of bladder cancer. Nat Rev Urol 16:613–630
6. Witjes JA, Bruins HM, Cathomas R, Comperat EM, Cowan NC, Gakis G et al (2021) European association of urology guidelines on muscle-invasive and metastatic bladder cancer: Summary of the 2020 guidelines. Eur Urol 79:82–104
7. Cumberbatch MGK, Jubber I, Black PC, Esperto F, Figueroa JD, Kamat AM et al (2018) Epidemiology of bladder cancer: a systematic review and contemporary update of risk factors in 2018. Eur Urol 74:784–795
8. Patel VG, Oh WK, Galsky MD (2020) Treatment of muscle-invasive and advanced bladder cancer in 2020. CA Cancer J Clin 70:404–423
9. Ngambenjawong C, Gustafson HH, Pun SH (2017) Progress in tumor-associated macrophage (TAM)-targeted therapeutics. Adv Drug Deliv Rev 114:206–221
10. Najafi M, Hashemi Goradel N, Farhood B, Salehi E, Nashtaei MS, Khanlarkhani N et al (2019) Macrophage polarity in cancer: a review. J Cell Biochem 120:2756–2765
11. Li X, Liu R, Su X, Pan Y, Han X, Shao C et al (2019) Harnessing tumor-associated macrophages as aids for cancer immunotherapy. Mol Cancer 18:177
12. Cioni B, Zaalberg A, van Beijnum JR, Melis MHM, van Burgsteden J, Muraro MJ et al (2020) Androgen receptor signalling in macrophages promotes TREM-1-mediated prostate cancer cell line migration and invasion. Nat Commun 11:4498
13. Mantovani A, Sozzani S, Locati M, Allavena P, Sica A (2002) Macrophage polarization: tumor-associated macrophages as a paradigm for polarized M2 mononuclear phagocytes. Trends Immunol 23:549–555
14. Fu H, Zhu Y, Wang Y, Liu Z, Zhang J, Xie H et al (2018) Identification and validation of stromal immunotype predict survival and benefit from adjuvant chemotherapy in patients with muscle-invasive bladder cancer. Clin Cancer Res 24:3069–3078
15. Hu B, Wang Z, Zeng H, Qi Y, Chen Y, Wang T et al (2020) Blockade of DC-SIGN(+) tumor-associated macrophages reactivates antitumor immunity and improves immunotherapy in muscle-invasive bladder cancer. Cancer Res 80:1707–1719
16. Qi Y, Chang Y, Wang Z, Chen L, Kong Y, Zhang P et al (2019) Tumor-associated macrophages expressing galectin-9 identify immunoevasive subtype muscle-invasive bladder cancer with poor prognosis but favorable adjuvant chemotherapeutic response. Cancer Immunol Immunother 68:2067–2080
17. Zeng H, Zhou Q, Wang Z, Zhang H, Liu Z, Huang Q, et al (2020) Stromal LAG-3(+) cells infiltration defines poor prognosis subtype muscle-invasive bladder cancer with immunoevasive contexture. J Immunother Cancer. 8.
18. Mariathasan S, Turley SJ, Nickles D, Castiglioni A, Yuen K, Wang Y et al (2018) TGFbeta attenuates tumour response to PD-L1 blockade by contributing to exclusion of T cells. Nature 554:544–548

19. Taber A, Christensen E, Lamy P, Nordentoft I, Prip F, Lindskrog SV et al (2020) Molecular correlates of cisplatin-based chemotherapy response in muscle invasive bladder cancer by integrated multi-omics analysis. Nat Commun 11:4858
20. Zeng H, Liu Z, Wang Z, Zhou Q, Qi Y, Chen Y et al (2020) Intratumoral IL22-producing cells define immunoevasive subtype muscle-invasive bladder cancer with poor prognosis and superior nivolumab responses. Int J Cancer 146:542–552
21. Salmaninejad A, Valilou SF, Soltani A, Ahmadi S, Abarghan YJ, Rosengren RJ et al (2019) Tumor-associated macrophages: role in cancer development and therapeutic implications. Cell Oncol (Dordr) 42:591–608
22. Gunesch JT, Dixon AL, Ebrahim TA, Berrien-Elliott MM, Tatineni S, Kumar T, et al (2020) CD56 regulates human NK cell cytotoxicity through Pyk2. Elife. 9
23. Levine AG, Mendoza A, Hemmers S, Moltedo B, Niec RE, Schizas M et al (2017) Stability and function of regulatory T cells expressing the transcription factor T-bet. Nature 546:421–425
24. Stark JM, Tibbitt CA, Coquet JM (2019) The metabolic requirements of Th2 cell differentiation. Front Immunol 10:2318
25. Scapini P, Marini O, Tecchio C, Cassatella MA (2016) Human neutrophils in the saga of cellular heterogeneity: insights and open questions. Immunol Rev 273:48–60
26. Lenis AT, Lec PM, Chamie K, Mshs MD (2020) Bladder cancer: a review. JAMA 324:1980–1991
27. Kamoun A, de Reynies A, Allory Y, Sjodahl G, Robertson AG, Seiler R et al (2020) A consensus molecular classification of muscle-invasive bladder cancer. Eur Urol 77:420–433
28. Powles T, Huddart RA, Elliott T, Sarker SJ, Ackerman C, Jones R et al (2017) Phase III, double-blind, randomized trial that compared maintenance Lapatinib versus placebo after first-line chemotherapy in patients with human epidermal growth factor receptor 1/2-positive metastatic bladder cancer. J Clin Oncol 35:48–55
29. Loriot Y, Necchi A, Park SH, Garcia-Donas J, Huddart R, Burgess E et al (2019) Erdafitinib in locally advanced or metastatic urothelial carcinoma. N Engl J Med 381:338–348
30. Chen L, Han X (2015) Anti-PD-1/PD-L1 therapy of human cancer: past, present, and future. J Clin Invest 125:3384–3391
31. Pathria P, Louis TL, Varner JA (2019) Targeting tumor-associated macrophages in cancer. Trends Immunol 40:310–327
32. DeNardo DG, Ruffell B (2019) Macrophages as regulators of tumour immunity and immunotherapy. Nat Rev Immunol 19:369–382
33. Lobo N, Mount C, Omar K, Nair R, Thurairaja R, Khan MS (2017) Landmarks in the treatment of muscle-invasive bladder cancer. Nat Rev Urol 14:565–574
34. Tan TZ, Rouanne M, Tan KT, Huang RY, Thiery JP (2019) Molecular subtypes of urothelial bladder cancer: results from a meta-cohort analysis of 2411 tumors. Eur Urol 75:423–432
35. Choi W, Porten S, Kim S, Willis D, Plimack ER, Hoffman-Censits J et al (2014) Identification of distinct basal and luminal subtypes of muscle-invasive bladder cancer with different sensitivities to frontline chemotherapy. Cancer Cell 25:152–165
36. Zeng D, Ye Z, Wu J, Zhou R, Fan X, Wang G et al (2020) Macrophage correlates with immunophenotype and predicts anti-PD-L1 response of urothelial cancer. Theranostics 10:7002–7014
37. Robertson AG, Kim J, Al-Ahmadie H, Bellmunt J, Guo G, Cherniack AD et al (2017) Comprehensive molecular characterization of muscle-invasive bladder cancer. Cell. 171:540–56